ACS OMEGA

Open Access

http://pubs.acs.org/journal/acsodf

Article

CO_2 and CO Capture on the ZnO Surface: A GCMC and Electronic Structure Study

Julia Silva Gordijo, Nailton Martins Rodrigues, and João B. L. Martins*

Cite This: *ACS Omega* 2023, 8, 46830−46840

Read Online

ACCESS | Metrics & More | Article Recommendations

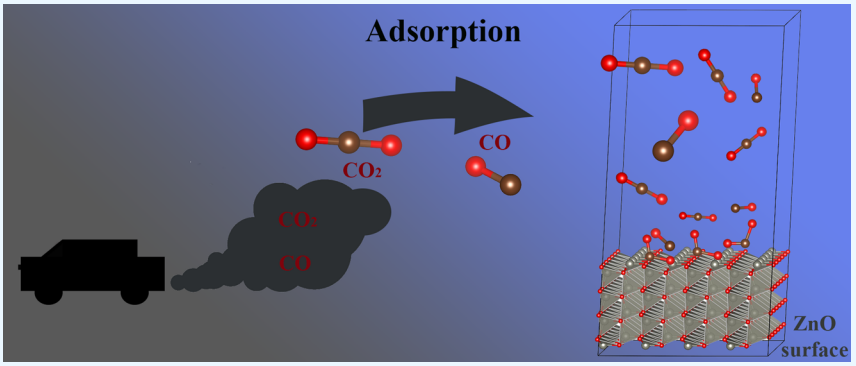

ABSTRACT: The amount of polluting gases released into the atmosphere has grown drastically. Among them, it is possible to cite the release of CO_2 and CO gases on a large scale as one of the products of the complete and incomplete combustion of petroleum-derived fuels. It is worth noting that the production of energy by burning fossil fuels supplies the energy demand but causes environmental damage, and several studies have addressed the reduction. One of them is using materials with the potential to capture these gases. The experimental and theoretical studies have significant contributions that promote advances in this area. Among the materials investigated, ZnO has emerged, demonstrating the considerable potential for capturing various gases, including CO_2 and CO. This work used density functional theory (DFT) and Grand Canonical Monte Carlo Method (GCMC) to investigate the adsorption of CO_2 and CO on the surface of Zinc oxide (ZnO) to obtain adsorption isotherms and interaction energy and the interaction nature. The results suggest that CO_2 adsorption slightly changed the angle of the O−C−O to values less than 180°. For the CO, its carbon atom interacts simultaneously with Zn and O of the ZnO surface. However, CO interactions have an ionic character with a lower binding energy value than the CO_2 interaction. The energies calculated using the PM6 and DFT methods generated results compatible with the experimental values. In applications involving a mixture of these two gases, the adsorption of CO_2 should be favored, and there may be inhibition of the adsorption of CO for high CO_2 concentrations.

1. INTRODUCTION

In the last decades, one can follow the growth of computational chemistry as a powerful technique in developing materials.[1,2] It can be used, for instance, in metal oxide adsorption investigations, which have been extensively researched due to their characteristics and potential for various applications. Zinc oxide (ZnO) is a semiconductor material with the most common hexagonal wurtzite structure.[3] The ZnO, which is a member of the VI family and has a variety of polar and nonpolar surfaces, has a widespread application in material science, one of which is derived from the high value of its bandgap (3.37 eV) and large exciton binding energy (60 meV).[4−6] Also, for use in medicinal and environmental applications, ZnO is biodegradable, biocompatible, and safe.[7] The ZnO usage is not limited but includes gas detection (due to its high sensitivity to various oxidizing gases and reducers),[8] electronic materials (such as photovoltaic cells and varistors),[9−11] and also catalysis (for the production of hydrogen from water, methanol synthesis, and hydrogenation of olefins, for example).[12] These and other ZnO applications have increased theoretical and experimental research on ZnO surfaces.[13−24]

Carbon dioxide is one of the leading greenhouse gases, and considering the growing concern with global climate changes, efforts to lower the atmospheric levels of this compound and transform it into less harmful molecules are of interest. In particular, for biofuel production as an alternative to fossil fuels,

Received: August 26, 2023
Revised: October 31, 2023
Accepted: November 10, 2023
Published: November 30, 2023

great attention has emerged in studying CO_2 adsorption and interaction in various substrates, including ZnO. Kinetic testing and Ambient Pressure Photoelectron Spectroscopy (AP-XPS) results show the critical role a ZnO-cover interface plays in synthesizing methanol from CO_2 hydrogenation.[25] Lately, the photochemical synthesis of methanol from CO_2 and H_2O molecules were demonstrated to be feasible on a ZnO surface using visible light, with ZnO proving to be a more efficient photocatalyst than $SrTiO_3$, TiO_2, and WO_3.[26] Furthermore, a recent study under density functional theory (DFT)-based simulations showed that using ZnO monolayers for CO_2 capture is viable. ZnO-ML presents a clear advantage compared to carbon nanotubes, graphene, and g-BN leaves.[27] This application is particularly promising for ZnO because as rising levels of CO_2 in the atmosphere are a severe concern for the health and future of the planet, there are strong economic and environmental incentives to look for ways to capture and turn CO_2 into raw materials for use in the chemical industry.

CO_2 capture/storage is a challenge for global warming, where several studies have been addressed for the adsorption of CO_2.[28−38] Studies of CO_2 capture show a maximum amount of CO_2 adsorbed ranging from approximately 25−176.66 mg/g at higher pressure.[35,39]

Carbon monoxide is a colorless, odorless, and toxic gas that is toxic for humans and animals. It has a high affinity for hemoglobin (long-term exposure should not exceed 25 ppm in 8 h or 50 ppm within 4 h).[40] This gas is not very soluble in water, which limits its removal from the air by water treatment. For this reason, CO_2 oxidation is a solution for reducing CO in air pollution treatments. However, to eliminate the CO, it is necessary to catalyze its oxidation. Upon adsorption, the catalyst concentrates the pollutant on its surface, which allows the oxidative reaction to proceed at a sufficient rate.[41] Catalytic oxidation of CO on ZnO surfaces has been extensively studied due to its importance in air pollution control and automotive exhaust treatment. Chen et al. studied CO oxidation over Au/ZnO and reported high catalytic activity for low-temperature CO oxidation below room temperature.[42] Adsorption and diffusion of CO on the polar surface of ZnO suggests that the presence of CO_2 enhances the binding of CO molecules.[43]

Additionally, recent studies have dealt with density functional theory (DFT) investigation of the gas−surface reactions.[44,45] In this context, it has been demonstrated in previous studies that zinc oxide can be effectively used as a sensor for various types of gases.[46−48] However, to control the selectivity of ZnO, it is vital to understand the interaction of the ZnO surface with the molecules of the gas adsorbed at the atomic level, which is still a considerable concern.

As stated, the adsorption of CO and CO_2 molecules on the ZnO surface is significant for many applications. It is also necessary before many catalytic operations, such as forming methanol from gas synthesis.[49−52] On metallic surfaces, the adsorption of gases like CO and CO_2 has been extensively studied.[53−56] In contrast, oxide surfaces have received much less attention. Moreover, there is a gap in the literature regarding CO and CO_2 adsorption isotherms on ZnO, especially for higher pressures. Theoretical investigations of zinc oxide surfaces are pertinent to achieving this requirement given the significance and variety of applications of zinc oxide. In this study, the adsorption isotherms for these gases on ZnO were obtained using the Grand Canonical Monte Carlo Method (GCMC). A rigorous model of adhesion at the molecular level is resolved using this GCMC statistical-mechanical method.[57] In order to comprehend the adsorbent−adsorbate interaction and the interaction between molecules of the adsorbent, adsorption energies were obtained using semiempirical methods and functional density theory (DFT), and the radial distribution function was analyzed with GCMC. This work investigates the interaction between the adsorbent and adsorbed molecules and the CO_2 and CO adsorption on a ZnO surface.

2. RESULTS AND DISCUSSION

2.1. CO_2 and CO Adsorption upon ZnO, Single Surface.

The adsorption of CO_2 and CO molecules on the ZnO surface was investigated, and adsorption isotherms were obtained on a single ZnO surface (4 layers). In order to compare the results, the simulations used different force fields to describe the gas molecule and the metal oxide surface. Adsorption was also assessed at 273.15, 298.15, and 323.15 K.

2.1.1. Carbon Dioxide. The isotherms obtained for CO_2 using the 4-layer model are shown in Figure 1. It can be noted

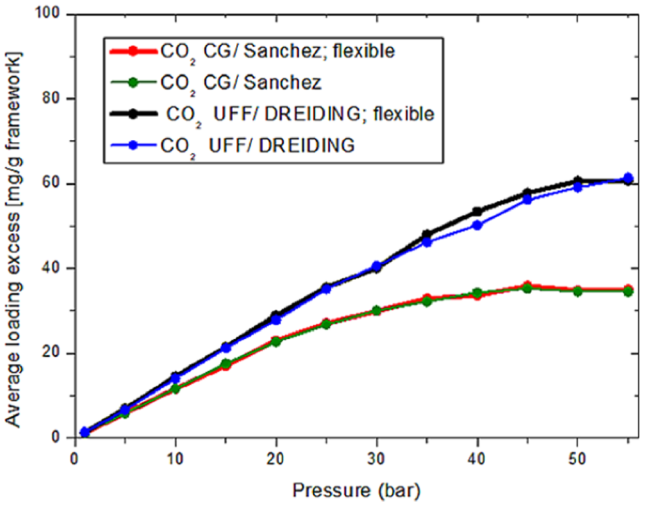

Figure 1. Excess adsorption isotherm of CO_2, flexible and rigid, on the ZnO surface at a temperature of 298 K achieved using different force fields. Sanchez and DREIDING for the gas and (CG) CrystalGenerator and (UFF) Universal force field for the ZnO atoms.

that the adsorption capacity increases with the pressure increase and the adsorption capability begins saturation around 50 bar. The values obtained for the adsorbed quantity vary according to the force field used. The best force field can be chosen by comparing it to experimental data. Data are only available for lower pressures, which opens up space for future experimental work in this field. The results obtained with the force fields CrystalGenerator (for ZnO) and Sanchez (gas) indicate a maximum CO_2 adsorption capacity of approximately 35 mg/g of adsorbent. Results obtained with the force fields UFF (for ZnO) and DREIDING (gas) estimate a higher maximum CO_2 adsorption capacity, approximately 60 mg/g of adsorbent.

Simulations were made with the flexible and rigid CO_2 molecule (Figure 1), and the analysis of the isotherms shows that the variation of the bonding angle does not influence the amount adsorbed. However, it can be seen that the isotherms obtained using the flexible molecules have a better trend near the saturation pressure. Figure 2 shows the adsorption isotherms for 273.15 298.15, and 323.15 K. These data allowed us to assess the temperature influence on adsorption.

https://doi.org/10.1021/acsomega.3c06378
ACS Omega 2023, 8, 46830−46840

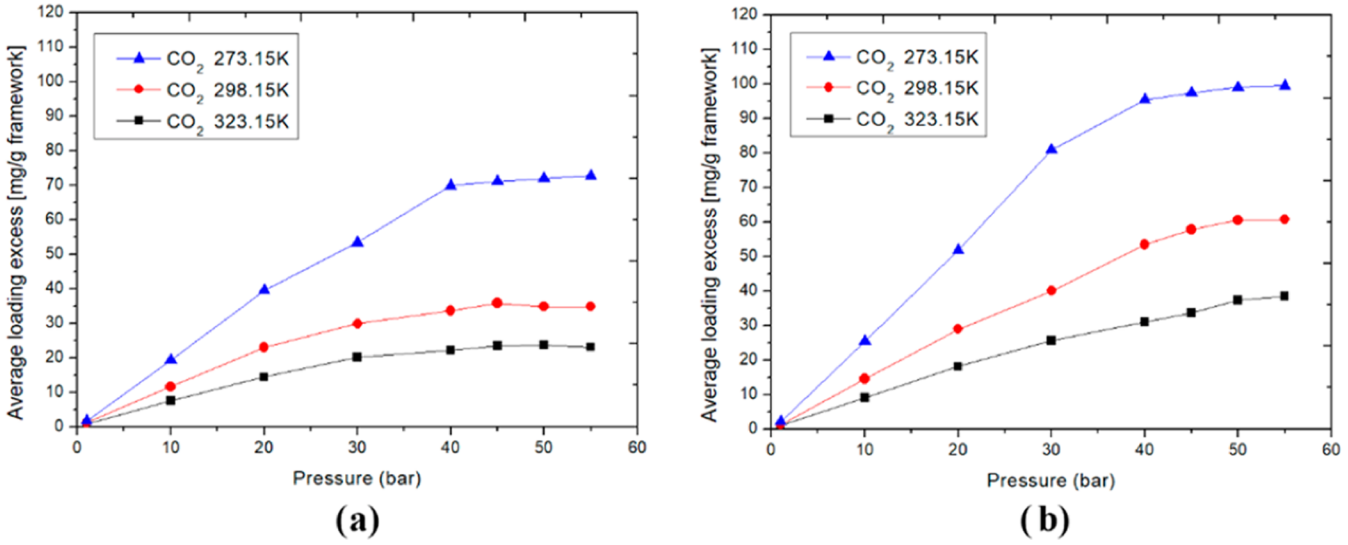

Figure 2. Excess adsorption isotherm of flexible CO_2 on the ZnO surface at temperatures of 273, 298, and 323 K using different force fields. (a) CrystalGenerator/Sanchez and (b) UFF/DREIDING.

As expected, the temperature heavily influences gas adsorption on the surface of ZnO. The literature reported an increase in the adsorption amount of CO_2 on ZnO with the decrease in temperature.[33,58] The adsorption at 25 bar reported a maximum value of about 133 mg/g ZnO at 373.15 K.[31] At low temperatures, the internal energy of the system is reduced; i.e., the gas molecules have less kinetic energy, enabling them to interact with available sites on the ZnO surface and increasing the adsorption capacity of the gas. At high temperatures, gas molecules have more kinetic energy. Therefore, the less likely interaction with the material surface reduces the adsorption capacity. Thus, using lower temperatures can boost the capacity of CO_2 adsorption into ZnO, with pressures above 30 bar not required, as the adsorption capacity with the pressure increases very little from this point.

Figure 3 shows the lateral interaction between CO_2···CO_2 molecules radial distribution functions (RDFs), considering a temperature of 278 K and pressures from 1 to 50 bar.

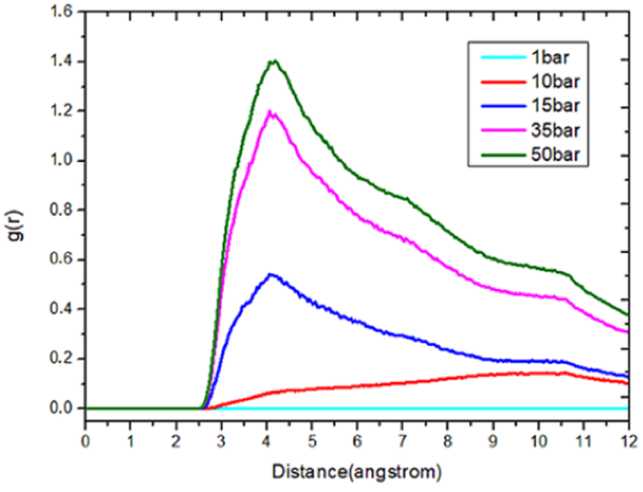

Figure 3. RDFs for the interaction between C_ CO_2 and O_CO_2 at a temperature of 298 K and 1, 10, 15, 35, and 50 bar pressures. O_CO_2 and C_CO_2 represent the oxygen and carbon of the CO_2 molecules, respectively.

The radial distribution shows that the minimum interaction distance between the CO_2 molecules is about 2.5 Å, and the interaction is more recurrent to the radial distance of approximately 4.18 Å, which can be observed by the peak in Figure 3 (first shell). Furthermore, it can be observed that the pressure significantly influences the shape of the radial distribution curve; i.e., only pressure above 15 bar has the peak distribution with distances of approximately 4.18 Å. Regarding the peak, it was possible to note that the higher the pressure, the greater the value of g(r), with interactions occurring more frequently for the pressure of 50 bar.

It was also analyzed the interaction between gas and ZnO atoms during adsorption using the RDF, and the results can be observed in Figure 4, which were obtained for a temperature of 278 K and pressures from 5 to 50 bar. The minimum interaction distance between CO_2 and ZnO is approximately 2.32 Å (Figure 4), slightly smaller than the one observed between the CO_2 molecule interaction.

Comparing the RDF data (Figure 4(a),(b)), a smaller interaction shell of Zn···O_CO_2 and O_ZnO···C_CO_2 was found at approximately 3.0 Å. It is understood that the interaction between O and C (of the CO_2 molecule) with the ZnO surface has quite a similar shape, suggesting no preference for the carbon or oxygen of CO_2 interacting with ZnO. This result is in line with a previous study indicating that both C and O of CO_2 may interact with the nonpolar surface of zinc oxide.[59] The peaks observed in Figure 4 show that the interaction between adsorbent and adsorbates has a maximum at a radial distance of around 7 Å (7.1 Å for the Zn−O_CO_2 interaction and about 7.26 Å for O_ZnO−C_CO_2). However, for the interaction among gas molecules (Figure 3), the most intense peak occurs at a shorter radial distance, indicating that multilayer adsorption is significant. In the interaction between adsorbent and adsorbates, it is realized that pressure significantly influences the shape of the radial distribution curve, and the interactions are more common for higher pressure (50 bar).

As expected, from the distribution density of the gas (Figure 5), the density map of adsorbed CO_2 is enhanced near the surface. There is an increase in the number of molecules adsorbed on the surface and in the region between layers from 5

https://doi.org/10.1021/acsomega.3c06378
ACS Omega 2023, 8, 46830−46840

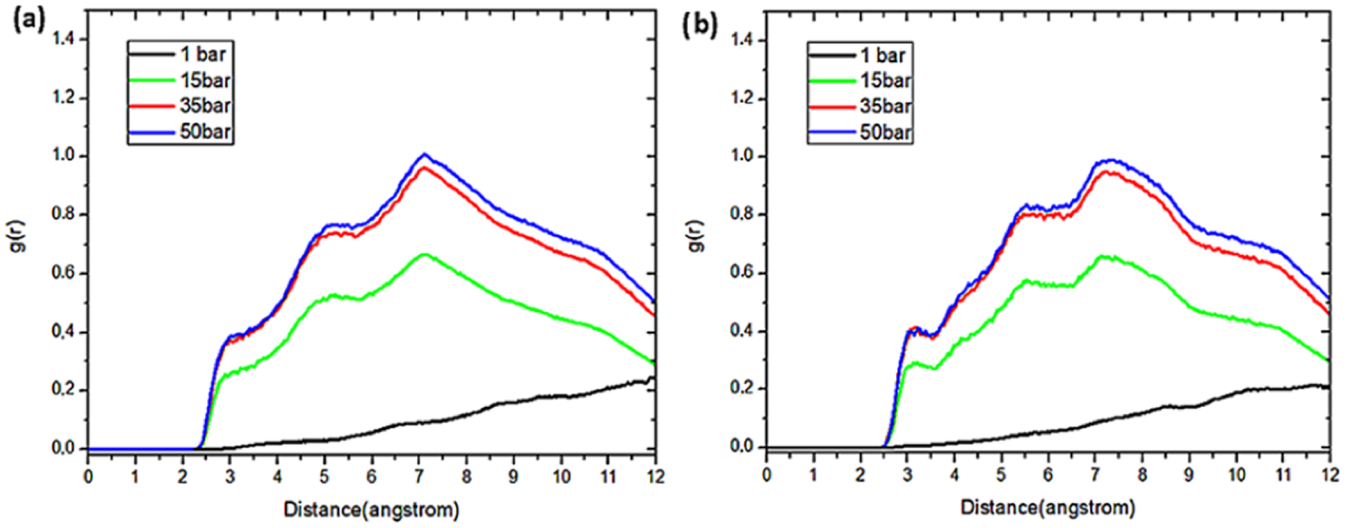

Figure 4. RDF for the interaction between (a) Zn and O_CO_2 and (b) O_ZnO and C_CO_2 at a temperature of 298 K and 1, 10, 15, 35, and 50 bar pressures. O_CO_2 and C_CO_2 represent the oxygen and the carbon of the CO_2 molecules, respectively, and O_ZnO represents the oxygen of the ZnO supercell.

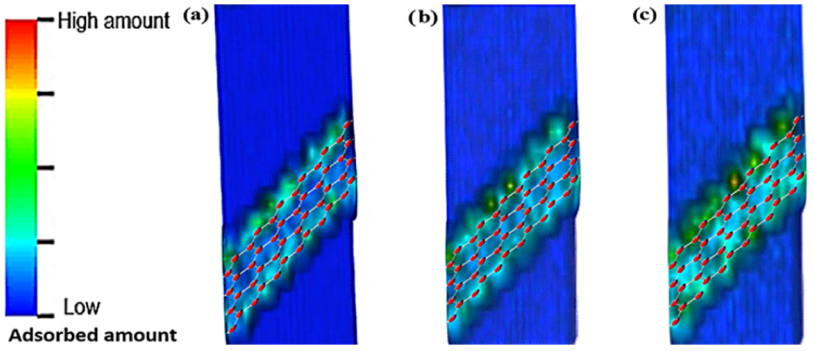

Figure 5. CO_2 distribution density map upon ZnO surfaces to (a) 5, (b) 25, and (c) 50 bar. For enhanced clarity, only one surface of ZnO is shown.

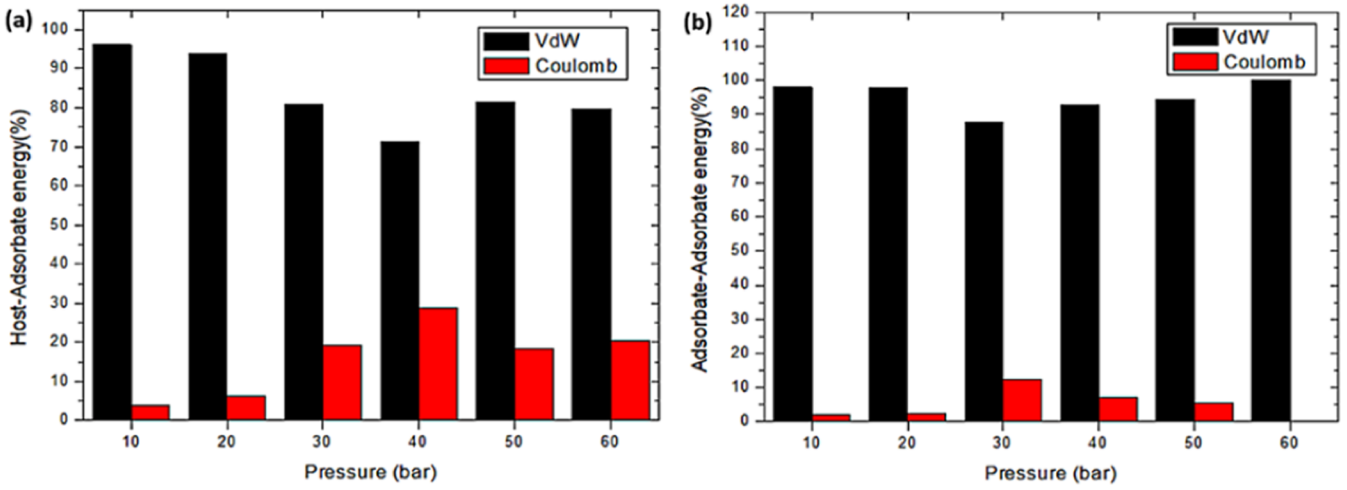

Figure 6. Variation of the interaction energies with pressure for adsorption of CO_2 upon ZnO: (a) host-adsorbate and (b) adsorbate−adsorbate at a temperature of 298 K.

to 50 bar (indicated by the change from blue to green, where blue = lower density and green = higher density).

The analysis of the average interaction energies between all molecules shows that although van der Waals-type interactions prevail, the Coulombic (stronger) interactions between CO_2 and the ZnO surface gain greater significance with increased pressure (Figure 6a). The energy of interaction between gas molecules follows a similar trend, but Coulomb-type interactions are less common and decrease considerably close to the saturation pressure (Figure 6b).

2.1.2. Carbon Monoxide (CO). For the CO molecule, the excess adsorption isotherm obtained at a temperature of 298 K is

https://doi.org/10.1021/acsomega.3c06378
ACS Omega 2023, 8, 46830−46840

shown in Figure 7. The saturation pressure for carbon monoxide adsorption on the surface of ZnO is approximately 190 bar,

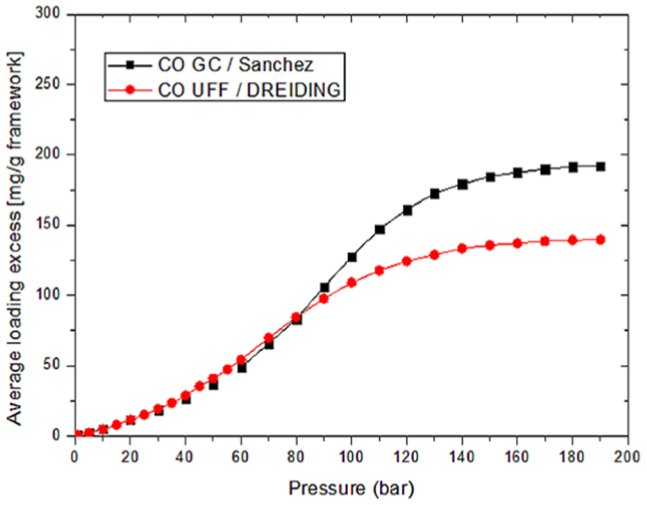

Figure 7. Excess adsorption isotherm of CO on the ZnO surface at a temperature of 298 K using different force fields. For the gas: Sanchez (GMOF) and DREIDING and for the ZnO atoms: (CG) CrystalGenerator and (UFF) Universal force field.

which is considerably higher than the saturation pressure obtained for the CO_2 molecules. The increase in the amount adsorbed with pressure becomes negligible at about 130 bar, so it should be assessed whether such high pressures are worthwhile.

The calculated maximum CO adsorption capacity was approximately 190 mg/g of adsorbent obtained using the force fields of CrystalGenerator (for ZnO) and Sanchez (gas) and 140 mg/g of adsorbent using the force fields of UFF (for ZnO) and DREIDING (gas).

Figure 8 shows the adsorption isotherm for different temperatures of CO. The analysis of the adsorption of CO on the surface of ZnO at various temperatures reveals that lower temperatures favor adsorption, the same trend found for CO_2. As illustrated in Figure 8, using temperatures near 273 K significantly increases the CO adsorption capability compared to room temperature. The saturation pressure is lower at this temperature, around 120 bar. Furthermore, a pressure of about 100 bar is recommended for low temperatures because the adsorption capacity is already virtually maximal at this pressure.

In terms of the RDF (Figure 9) at an optimum pressure of 130 bar, it was observed that the interaction of the CO molecule with

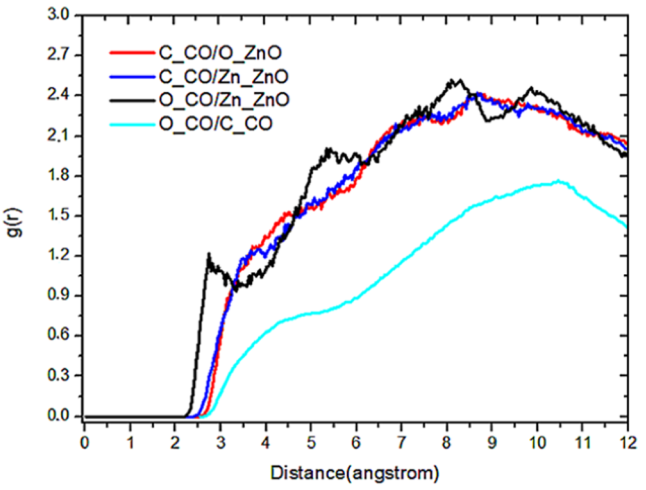

Figure 9. RDFs for the interaction between the ZnO surface and the CO gas and between the gas molecules at a temperature of 298 K and pressure of 130 bar.

the ZnO surface (Figure 9) appears to be more favored at long distances (7−10 Å). Moreover, there is evidence that the gas preferentially interacts with the Zn atom on the surface. Between the oxygen of the CO and the zinc of the ZnO surface, a minimum contact distance of around 2.0 Å was obtained. This distance is roughly 2.5 Å (significantly larger) for the interaction of gas with surface oxygen. There were no pronounced peaks in the RDF.

Similarly to that of CO_2, the distribution density of the CO gas (Figure 10) shows that, as expected, the density map of the

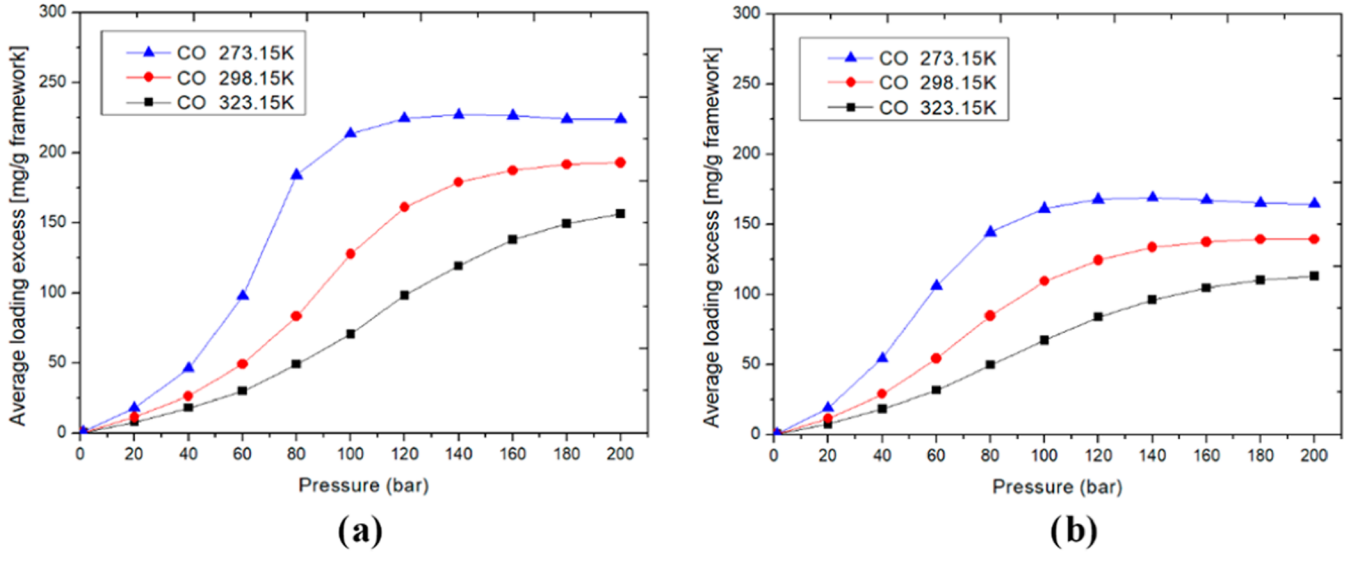

Figure 8. Excess adsorption isotherm of CO on the ZnO surface at temperatures of 273, 298, and 323 K using different force fields. (a) CrystalGenerator/Sanchez and (b) UFF/DREIDING.

https://doi.org/10.1021/acsomega.3c06378
ACS Omega 2023, 8, 46830−46840

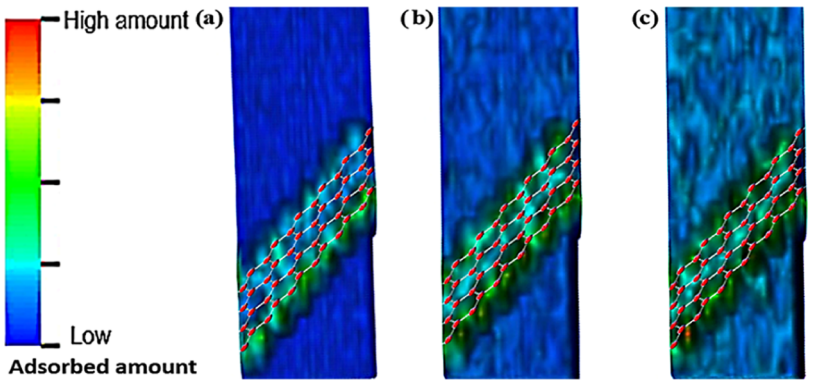

Figure 10. CO distribution density map upon ZnO surfaces to (a) 10, (b) 90, and (c) 180 bar. For enhanced clarity, only one surface of ZnO is shown.

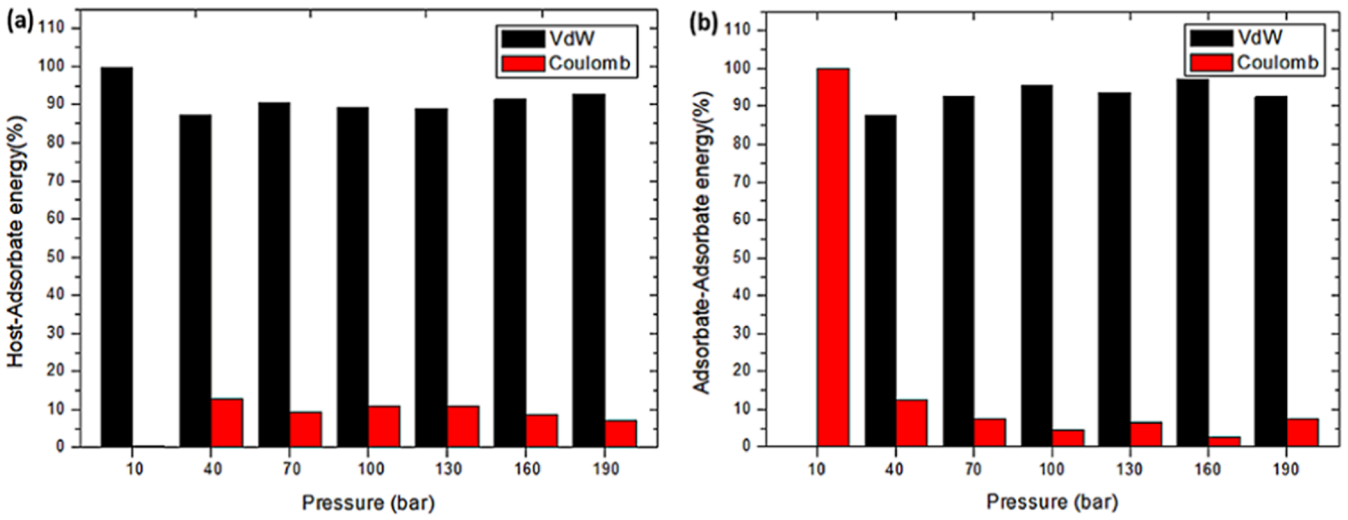

Figure 11. Variation of the interaction energies with pressure for adsorption of CO adsorption upon ZnO: (a) host−adsorbate and (b) adsorbate−adsorbate at a temperature of 298 K.

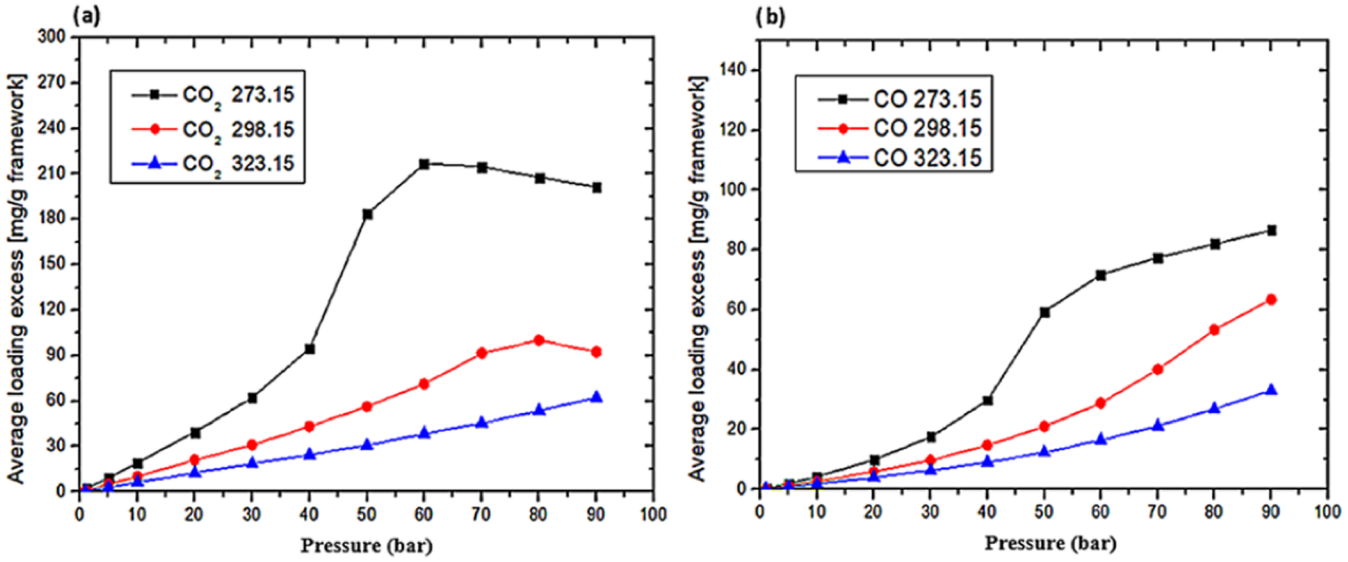

Figure 12. Comparison of the adsorption isotherms of (a) CO_2 and (b) CO for a mixture of 50% CO_2 and 50% CO at temperatures of 298, 273, and 323 K and different pressures.

adsorbed CO is more intense near the surface and that increasing pressure increases the number of absorbed molecules, both on the surface and in the layer-to-layer region (indicated by the change from blue to green, where blue = lower density and green = higher density).

The average interaction energies between all the molecules (Figure 11) show that at 10 bar, the interaction between CO and

https://doi.org/10.1021/acsomega.3c06378
ACS Omega 2023, 8, 46830−46840

the surface is purely van der Waals type (Figure 11a). In contrast, the interactions between gas molecules are purely Coulombic. However, the Coulombic interactions between CO molecules become less frequent as the pressure increases, decaying rapidly at first and then more slowly. At higher pressures, van der Waals interactions between the host and adsorbent remain dominant, but Coulombic interactions between CO and the ZnO surface become significant (Figure 11a).

2.1.3. Adsorption of a 50% CO_2 and 50% CO Mixture. In order to improve the quantitative study of the CO and CO_2 adsorption upon ZnO, adsorption at 50% CO_2 and 50% CO mixture were done. Simulations were made to quantify the adsorption of an equimolar mixture of both gases and analyze which gas prefers to adsorb on the surface. The combination of the Sanchez and CrystalGenerator force fields has been used, as they are more specific force fields for studies involving gas adsorption.

The isotherms obtained for temperatures of 273.15, 298.15, and 323.15 K are shown in Figure 12. The temperature shows no influence on the adsorption preference. Thus, in applications involving a CO_2/CO mixture, CO_2 adsorbs preferably over CO at all temperatures. However, it should be considered that CO_2 saturates before CO, so the use of pressures above 80 bar can allow extra adsorption of CO. This is also an indication that CO and CO_2 interact in different sites on the surface of ZnO since when there is surface saturation by CO_2, there is still increasing adsorption of CO.

Another point to consider is that the amount of CO_2 adsorbed increases considerably in the presence of CO, comparing the isotherm for the equimolar mixture of CO and CO_2 at 298 K (Figure 12) with the adsorption isotherm for pure CO_2 at the same temperature obtained using the same force fields (Figure 1). The presence of CO significantly increases the maximum amount of CO_2 adsorption from 35 mg/g at a saturation pressure of 50 bar to about 110 mg/g and a saturation pressure of 80 bar. Results in the literature are for the very low-pressure regime, showing an increase in the CO strength with coadsorbed CO_2.[43,60] These findings are correlated to the structures observed in the electronic calculations of the next section.

2.2. CO_2 and CO Adsorption Energies on the Surface of ZnO and Related Properties. The PM6, PM6-D3, PM7, semiempirical methods, and DFT using B3LYP functional calculations with counterpoise correction have been used to study the interaction of CO and CO_2 molecules with the ZnO surface and evaluate the reliability of semiempirical methods. Two modes were studied for CO and CO_2 (Figure 13). Mode I is monodentated, and mode II is bidentated. CO_2 equilibrium reaction over ZnO forming carbonate Mode II (Figure 13) was experimentally reported.[11]

The configurations found for the interaction of CO_2 and CO with the surface are shown in Figure 13. The results of DFT optimization, in which the molecules would be free to interact in mode I or II, indicate a unique preferential mode of interaction between gases and ZnO. For the CO interacting linearly with zinc by the end of the carbon, Mode I is preferential for the ZnO−CO interaction. For CO_2 making a bridge between two Zn atoms (bidentate), Mode II is the preferential interaction for ZnO−CO_2. The semiempirical results under these conditions also confirm this trend, and the adsorption energies for these modes of interaction obtained with PM6 are in accordance with the values found in the literature and obtained experimentally. Thus, CO is absorbed linearly through the end of the carbon. At

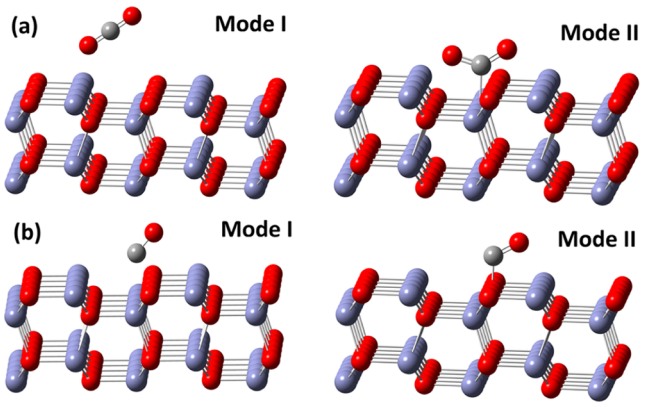

Figure 13. (a) Interaction between CO_2 and the ZnO surface. (b) Interaction between CO and the surface of ZnO. Gray, zinc; red, oxygen; and brown, carbon. Results of PM6 (semiempirical) calculations.

the same time, CO_2 adsorbs on the surface with both carbon and oxygen atoms interacting with ZnO, and in this interaction, the O−C−O angle of the molecule becomes 132.45°. The mode of interaction with linear CO_2 is energetically less favored. The bidentate configuration for CO (Mode II) generates a higher adsorption energy.

The adsorption energy values are shown in Table 1. The calculated energies using the PM6 and DFT methods generated

Table 1. Adsorption Energies (kcal/mol) for CO and CO_2 on the ZnO Surface Calculated by Using Different Methods[a]

	adsorption energy (kcal/mol)			
method	CO_2 (mode I)	CO_2 (mode II)	CO (mode I)	CO (mode II)
PM6	−5.712	−36.901	−11.558	−71.849
PM6-D3	−11.530	−40.689	−16.016	−77.273
PM7	−5.877	−61.515	−21.153	−66.484
DFT		−71.610	−10.380	

[a]CO_2 and CO have only shown Mode II and I of interaction using the B3LYP functional, respectively.

results compatible with the experimental value of −12 kcal/mol[61,62] for CO, mode I. Mode II of CO is related to the chemisorption of CO coming from CO_2 formation and is expected with a higher interaction energy due to the bonding formation.[59,63] The result obtained by the PM6 method for CO_2 is consistent with the experimental value of −33.5 kcal/mol.[63] However, the PM6-D3 and PM7 semiempirical methods, and even the DFT method, tend to overestimate these values for both molecules. The CO_2 adsorption energy is considerably more significant than the CO on the ZnO surface, about three times according to the semiempirical methods and six times by the DFT results (between 3 and 4 times greater experimentally). This result is evidence that CO_2 adsorption is more favored and explains why the surface of ZnO saturates at lower pressures when compared with the CO isotherms. Therefore, in applications involving a mixture of these two gases, the adsorption of CO_2 should be favored, and there may be inhibition of CO adsorption for high CO_2 concentrations. The result is consistent with the isotherm analysis for a mixture of both gases (Figure 12).

DFT of the most favorable interaction was used for the NCI calculations. For CO_2, two interactions are made with the ZnO surface and have distinct characteristics. The interaction

https://doi.org/10.1021/acsomega.3c06378
ACS Omega 2023, 8, 46830−46840

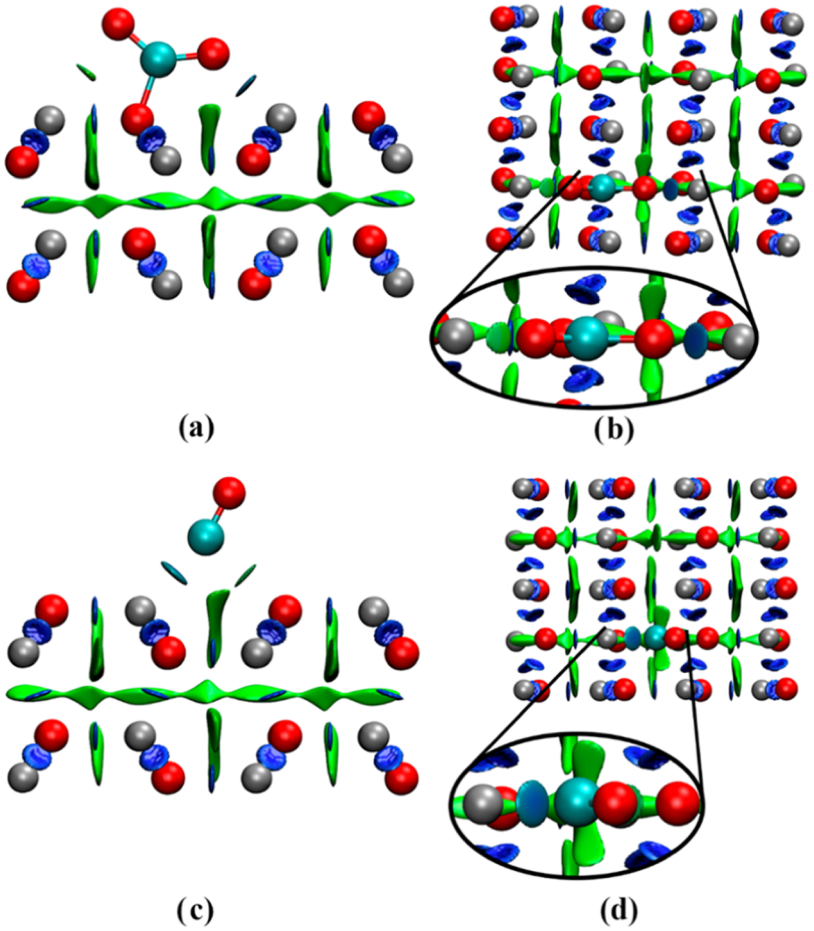

Figure 14. NCI for the interaction of CO and CO_2 molecules with the ZnO surface and the minimum energy point obtained with DFT. (a) CO_2−ZnO side view, (b) CO_2−ZnO upper view, (c) CO−ZnO side view, and (d) CO−ZnO upper view.

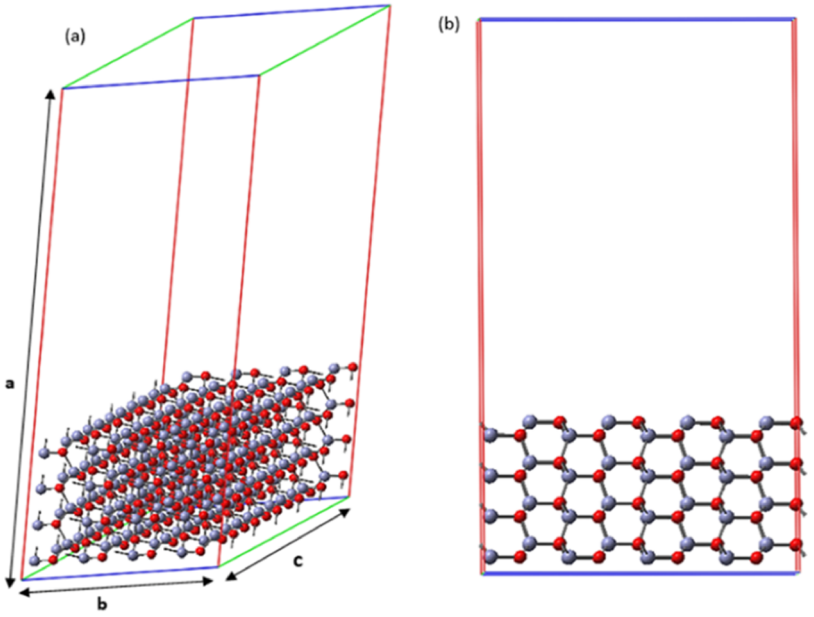

Figure 15. Simulation box used for obtaining the adsorption isotherms. (a) Box dimensions. (b) box with the ZnO surface, bulk structure with 4 layers.

between the carbon of CO_2 and the oxygen from the surface forms one covalent bond. The other has a strong electrostatic character (tone of blue in the region between atoms) and is generated by the interaction between an oxygen atom and a zinc atom on the surface (Figure 14a,14b).

The NCI results for CO (Figure 14c,14d) demonstrated that the carbon atom of the molecule interacts simultaneously with

https://doi.org/10.1021/acsomega.3c06378
ACS Omega 2023, 8, 46830−46840

zinc and oxygen atoms on the surface and that the interaction with zinc has a mild electrostatic character (light blue). In contrast, the interaction with oxygen has a weaker van der Waals character (the green region between these atoms).

3. CONCLUSIONS

Grand Canonical Monte Carlo, semiempirical (PM6, PM6-D3, and PM7), and DFT (B3LYP/6-31++G**) methods were used to study the adsorption and capture of CO_2 and CO on the ZnO nonpolar surface. Simulations of the isotherms of CO_2 show a maximum adsorption capacity of approximately 60 mg/g. Simulations were made with the rigid and flexible CO_2 molecule, and the analysis of the isotherms showed that the variation of the bonding angle does not influence the amount adsorbed. Lower temperatures can boost the capacity of adsorption of CO_2 into ZnO, with pressures above 30 bar not required, as the adsorption capacity with the pressure increases very little from this point. The radial distribution shows that the minimum interaction distance between the CO_2 molecules is about 2.5 Å and the interaction is more recurrent to the radial distance of approximately 4.18 Å. Although van der Waals-type interactions prevail, the Coulombic interactions (stronger) between CO_2 and the ZnO surface gain greater significance with increased pressure. The saturation pressure for carbon monoxide adsorption on the surface of ZnO is approximately 190 bar, considerably higher than the saturation pressure obtained for CO_2 molecules. At higher pressures, van der Waals interactions between the host and adsorbent remain dominant, but Coulombic interactions between the CO and the ZnO surface become significant. In an equimolar mixture of both gases, CO_2 adsorbs preferably over CO at all temperatures, and the presence of CO significantly increases the maximum amount of CO_2 adsorption. The energies calculated using the PM6 and DFT methods generated results compatible with the experimental values. In applications involving a mixture of these two gases, the adsorption of CO_2 should be favored, and there may be inhibition of CO adsorption for high CO_2 concentrations.

4. METHODOLOGY

This study used ZnO as a two-dimensional supercell for the adsorption on a four-layer ZnO surface with lattice parameters: a = 45.00, b = 19.74, and c = 21.23 Å (Figure 15). Cell parameter a was defined as 45.00 Å to prevent interactions between surfaces of the simulation box. The surface used for the study was the nonpolar ZnO surface ($10\bar{1}0$), the most stable face.[64−68] The gases were modeled using the Molden5.7 program,[69] and the equilibrium geometries were obtained from DFT calculations using the B3LYP functional and the 6-311++G** basis set through the Gaussian09 program package.[70]

Adsorption isotherms on the ZnO surface were obtained at a temperature of 278 K and different pressures using 50,000 simulation cycles for each studied pressure. For this process, GCMC simulations were made using the RASPA program.[71] From the GCMC simulation, the radial distribution functions (RDF) for the interaction between the gas molecules (lateral interactions) and interactions among the gases and ZnO surface, and the distribution density of the gas molecules along the entire simulation were obtained. The simulation box is depicted in Figure 15. The structure of ZnO was kept fixed during the simulation, and the gas geometry possessed total freedom in its translational and rotational modes. For CO_2, simulations with the flexible gas molecule were also carried out to assess whether changes in the OCO bonding angle influence adsorption.

ZnO partial charges were calculated by the Wilmer and Snurr method[72] in the RASPA program. For the gases, the charge for each atom had previously been obtained by ChelpG calculations in the Gaussian09 program. Because atoms were kept fixed during the simulation, it was possible to consider only nonbonded interactions. Then, only Lennard-Jones parameters (σ and ε/k_B, with k_B being the Boltzmann constant) were used for each atom. The Lorentz−Berthelot method described in eqs 1 and 2 was used to study the interactions with different atoms. The Coulomb potential resulting from charge interactions was calculated using the Ewald method.[73]

$$\sigma_{ab} = \frac{\sigma_a + \sigma_b}{2} \quad (1)$$

$$\varepsilon_{ab} = \sqrt{\varepsilon_a \varepsilon_b} \quad (2)$$

In order to compare the results, the atoms of CO_2, CO, and ZnO were treated with different force fields. Sanchez and DREIDING force fields were used for the gas. The ZnO atoms were described through the CrystalGenerator and UFF force fields contained in the RASPA program. Tables 2 and 3 list the force field parameters used in the simulation and their corresponding atoms.

Table 2. Lennard-Jones Parameters (Nonbond Parameters) for the Atoms used in the GCMC Simulation for Different Force Fields: CrystalGenerator (CG), Universal force field (UFF), Sanchez and DREIDING

	ZnO CG		ZnO UFF	
atom	σ (Å)	ξ/k_b (K)	σ (Å)	ξ/k_b (K)
Zn	2.46155	62.3992	2.763	62.40
O	3.03315	48.1581	3.50	30.193
	CO_2 Sanchez		CO_2 DREIDING	
atom	σ (Å)	ξ/k_b (K)	σ (Å)	ξ/k_b (K)
C	2.80	27.0	3.47	47.86
O	3.05	79.0	3.03	48.19
	CO Sanchez		CO DREIDING	
atom	σ (Å)	ξ/k_b (K)	σ (Å)	ξ/k_b (K)
C	3.296	60.39	3.47	47.86
O	2.85	100.65	3.03	48.19

Table 3. Force Field Parameters CO_2 flexible (Bond Parameters)

C−O bond		O−C−O angle	
k_{CO} (K/Å^2)	$r_{0\ CO}$ (Å)	k_{OCO} (K/rad^2)	$\theta_{0\ OCO}$ (deg)
1,015,500.0	1.162	54,351.4	180.0

The adsorption energies calculations were performed in the MOPAC2016 program[74] using the semiempirical methods PM6, PM6-D3, and PM7, and the large supercell comprising $(ZnO)_{50}$, while the Gaussian09 program[70] was used for DFT with B3LYP functional and 6-31++G** basis function for the small supercell of $(ZnO)_{20}$.

■ ASSOCIATED CONTENT

Data Availability Statement

All data and information for the reproduction of these works are available in the text.

https://doi.org/10.1021/acsomega.3c06378
ACS Omega 2023, 8, 46830−46840

AUTHOR INFORMATION

Corresponding Author

João B. L. Martins − *Universidade de Brasília, Instituto de Química, 70910-900 Brasília, DF, Brazil;* orcid.org/0000-0001-8677-3239; Email: lopes@unb.br

Authors

Julia Silva Gordijo − *Universidade de Brasília, Instituto de Química, 70910-900 Brasília, DF, Brazil*

Nailton Martins Rodrigues − *Universidade de Brasília, Instituto de Química, 70910-900 Brasília, DF, Brazil;* orcid.org/0000-0003-0597-0375

Complete contact information is available at: https://pubs.acs.org/10.1021/acsomega.3c06378

Author Contributions

Conceptualization: J.S.G.; J.B.L.M.; N.M.R. Methodology: J.S.G.; N.M.R.; J.B.L.M. Validation: J.S.G.; N.M.R. Formal analysis: J.S.G.; N.M.R.; J.B.L.M. Investigation: J.S.G.; N.M.R. Resources: J.S.G.; N.M.R.; J.B.L.M. Data Curation: J.S.G.; N.M.R. Whiting: J.S.G.; N.M.R. Review: N.M.R.; J.B.L.M. Visualization: J.S.G.; N.M.R.; J.B.L.M. Supervision: N.M.R.; J.B.L.M. Project administration: N.M.R. Funding acquisition: N.M.R.; J.B.L.M.

Funding

Brazilian agencies CAPES, CNPQ, and FAPDF (00193−00000926/2021−81) supported the research.

Notes

The authors declare no competing financial interest.

ACKNOWLEDGMENTS

We acknowledge the financial support from the Brazilian agencies CAPES, CNPq, and FAPDF (00193-00000926/2021-81).

REFERENCES

(1) Rodrigues, N. M.; Politi, J. R. S.; Martins, J. B. L. Are metal dopant and ligands efficient to optimize the adsorption rate of CH4, H2 and H2S on IRMOFs? Insights from factorial design. *Comput. Mater. Sci.* **2022**, *210*, No. 111438.

(2) de Araujo Oliveira, A. L.; de Macedo, L. G. M.; de Oliveira Só, Y. A.; Martins, J. B. L.; Pirani, F.; Gargano, R. Nature and role of the weak intermolecular bond in enantiomeric conformations of H2O2−noble gas adducts: a chiral prototypical model. *New J. Chem.* **2021**, *45*, 8240−8247.

(3) Mehrabian, M.; Azimirad, R.; Mirabbaszadeh, K.; Afarideh, H.; Davoudian, M. UV detecting properties of hydrothermal synthesized ZnO nanorods. *Phys. E* **2011**, *43*, 1141−1145.

(4) Viswanath, R. N.; Ramasamy, S.; Ramamoorthy, R.; Jayavel, P.; Nagarajan, T. Preparation and characterization of nanocrystalline ZnO based materials for varistor applications. *Nanostruct. Mater.* **1995**, *6*, 993−996.

(5) Kalpana, V. N.; Rajeswari, V. D. A Review on Green Synthesis, Biomedical Applications, and Toxicity Studies of ZnO NPs. *Bioinorg. Chem. Appl.* **2018**, *2018*, No. 3569758.

(6) Vasei, H. V.; Masoudpanah, S. M.; Adeli, M.; Aboutalebi, M. R. Solution combustion synthesis of ZnO powders using various surfactants as fuel. *J. Sol−Gel Sci. Technol.* **2019**, *89*, 586−593.

(7) Zhou, J.; Xu, N. S.; Wang, Z. L. Dissolving Behavior and Stability of ZnO Wires in Biofluids: A Study on Biodegradability and Biocompatibility of ZnO Nanostructures. *Adv. Mater.* **2006**, *18*, 2432−2435.

(8) Zeng, Y.; Zhang, T.; Yuan, M.; Kang, M.; Lu, G.; Wang, R.; Fan, H.; He, Y.; Yang, H. Growth and selective acetone detection based on ZnO nanorod arrays. *Sens. Actuators, B* **2009**, *143*, 93−98.

(9) Hohenberger, G.; Tomandl, G.; Ebert, R.; Taube, T. Inhomogeneous Conductivity in Varistor Ceramics: Methods of Investigation. *J. Am. Ceram. Soc.* **1991**, *74*, 2067−2072.

(10) Wenas, W. W.; Yamada, A.; Takahashi, K.; Yoshino, M.; Konagai, M. Electrical and optical properties of boron-doped ZnO thin films for solar cells grown by metalorganic chemical vapor deposition. *J. Appl. Phys.* **1991**, *70*, 7119−7123.

(11) Levinson, L.; Philipp, H. ZnO Varistors for Transient Protection. *IEEE Trans. Parts, Hybrids, Packag.* **1977**, *13*, 338−343.

(12) Wang, J.; Burghaus, U. Adsorption dynamics of CO2 on Zn-ZnO(0001): a molecular beam study. *J. Chem. Phys.* **2005**, *122*, No. 044705.

(13) Solomon, E. I.; Jones, P. M.; May, J. A. Electronic structures of active sites on metal oxide surfaces: definition of the copper-zinc oxide methanol synthesis catalyst by photoelectron spectroscopy. *Chem. Rev.* **1993**, *93*, 2623−2644.

(14) Jaffe, J. E.; Harrison, N. M.; Hess, A. C. Ab initio study of ZnO (101-bar0) surface relaxation. *Phys. Rev. B* **1994**, *49*, 11153−11158.

(15) Schroer, P.; Kruger, P.; Pollmann, J. Self-consistent electronic-structure calculations of the (101-bar0) surfaces of the wurtzite compounds ZnO and CdS. *Phys. Rev. B* **1994**, *49*, No. 17092.

(16) Martins, J. B. L.; Longo, E.; Andrés, J.; Taft, C. A. CO interaction with ZnO surfaces: an MNDO, AM1 and PM3 theoretical study with large cluster models. *J. Mol. Struct.: THEOCHEM* **1996**, *363*, 249−256.

(17) Martins, J. B. L.; Taft, C. A.; Longo, E.; Andres, J. Ab initio study of CO and H2 interaction on ZnO surfaces using a small cluster model. *J. Mol. Struct.: THEOCHEM* **1997**, *398*−*399*, 457−466.

(18) Martins, J. B. L.; Taft, C. A.; Longo, E.; de Castro, E. A. S.; da Cunha, W. F.; Politi, J. R. S.; Gargano, R. ONIOM study of dissociated hydrogen and water on ZnO surface. *Int. J. Quantum Chem.* **2012**, *112*, 3223−3227.

(19) Moraes, E.; Gargano, R.; Politi, J.; Castro, E.; Santos, J.; Longo, E.; Taft, C.; Martins, J. A Theoretical Investigation of ZnO Nanotubes: Size and Diameter. *Curr. Phys. Chem.* **2013**, *3*, 400−407.

(20) de Lima, Í. P.; dos S Politi, J. R.; Gargano, R.; Martins, J. B. L. Lateral interaction and spectroscopic constants of CO adsorbed on ZnO. *Theor. Chem. Acc.* **2015**, *134*, No. 49.

(21) Martins, J. B. L.; Longo, E.; Tostes, J. G. R.; Taft, C. A.; Andres, J. Quantum chemical study of the adsorption of water on zinc oxide surface. *J. Mol. Struct.: THEOCHEM* **1994**, *303*, 19−24.

(22) Martins, J. B. L.; Longo, E.; Salmon, O. D. R.; Espinoza, V. A. A.; Taft, C. A. The interaction of H2, CO, CO2, H2O and NH3 on ZnO surfaces: an Oniom Study. *Chem. Phys. Lett.* **2004**, *400*, 481−486.

(23) Martins, J. B. L.; Taft, C. A.; Lie, S. K.; Longo, E. Lateral interaction of CO and H 2 molecules on ZnO surfaces: an AM1 study. *J. Mol. Struct.: THEOCHEM* **2000**, *528*, 161−170.

(24) Martins, J. B. L.; Longo, E.; Taft, C. A.; Andrés, J. Ab initio and semiempirical MO studies using large cluster models of CO and H2 adsorption and dissociation on ZnO surfaces with the formation of ZnH and OH species. *J. Mol. Struct.: THEOCHEM* **1997**, *397*, 147−157.

(25) Palomino, R. M.; Ramirez, P. J.; Liu, Z.; Hamlyn, R.; Waluyo, I.; Mahapatra, M.; Orozco, I.; Hunt, A.; Simonovis, J. P.; Senanayake, S. D.; Rodriguez, J. A. Hydrogenation of CO(2) on ZnO/Cu(100) and ZnO/Cu(111) Catalysts: Role of Copper Structure and Metal-Oxide Interface in Methanol Synthesis. *J. Phys. Chem. B* **2018**, *122*, 794−800.

(26) Watanabe, M. Photosynthesis of methanol and methane from CO2 and H2O molecules on a ZnO surface. *Surf. Sci. Lett.* **1992**, *279*, L236−L242.

(27) Rao, G. S.; Hussain, T.; Islam, M. S.; Sagynbaeva, M.; Gupta, D.; Panigrahi, P.; Ahuja, R. Adsorption mechanism of graphene-like ZnO monolayer towards CO(2) molecules: enhanced CO(2) capture. *Nanotechnology* **2016**, *27*, No. 015502.

(28) Chai, S. Y. W.; Ngu, L. H.; How, B. S. Review of carbon capture absorbents for CO 2 utilization. *Greenhouse Gases: Science and Technology* **2022**, *12*, 394−427.

(29) Daud, N. K.; Muthiyah, D. Adsorption of CO2 on Activated Carbon, Fe-Based Metal Organic Framework, ZnO, and CaO for

https://doi.org/10.1021/acsomega.3c06378
ACS Omega 2023, 8, 46830−46840

Carbon Capture and Storage Application *Chem. Eng. Technol.* 2023, DOI: 10.1002/ceat.202200552.
(30) Ghosh, S.; Ranjan, P.; Ramaprabhu, S.; Sarathi, R. Carbon Dioxide Adsorption of Zinc Oxide Nanoparticles Synthesized by Wire Explosion Technique. *INAE Lett.* **2018**, *3*, 197−202.
(31) Kumar, S. The effect of elevated pressure, temperature and particles morphology on the carbon dioxide capture using zinc oxide. *J. CO2 Util.* **2014**, *8*, 60−66.
(32) Xia, X.; Strunk, J.; Busser, W.; Naumann d'Alnoncourt, R.; Muhler, M. Probing the Surface Heterogeneity of Polycrystalline Zinc Oxide by Static Adsorption Microcalorimetry. 1. The Influence of the Thermal Pretreatment on the Adsorption of Carbon Dioxide. *J. Phys. Chem. C* **2008**, *112*, 10938−10942.
(33) Smyrnioti, M.; Tampaxis, C.; Steriotis, T.; Ioannides, T. Study of CO2 adsorption on a commercial CuO/ZnO/Al2O3 catalyst. *Catal. Today* **2020**, *357*, 495−502.
(34) Anuar, S. A.; Ahmad, K. N.; Al-Amiery, A.; Masdar, M. S.; Wan Isahak, W. N. R. Facile Preparation of Carbon Nitride-ZnO Hybrid Adsorbent for CO2 Capture: The Significant Role of Amine Source to Metal Oxide Ratio. *Catalysts* **2021**, *11*, No. 1253.
(35) Fernandez, D. C.; Morales, D. S.; Jiménez, J. R.; Fernández-Rodriguez, J. M. CO2 adsorption by organohydrotalcites at low temperatures and high pressure. *Chem. Eng. J.* **2022**, *431*, No. 134324.
(36) Gouvêa, D.; Ushakov, S. V.; Navrotsky, A. Energetics of CO2 and H2O adsorption on zinc oxide. *Langmuir* **2014**, *30*, 9091−9097.
(37) Gouveia, L. G. T.; Agustini, C. B.; Perez-Lopez, O. W.; Gutterres, M. CO2 adsorption using solids with different surface and acid-base properties. *J. Environ. Chem. Eng.* **2020**, *8*, No. 103823.
(38) Burghaus, U. Surface science perspective of carbon dioxide chemistry—Adsorption kinetics and dynamics of CO2 on selected model surfaces. *Catal. Today* **2009**, *148*, 212−220.
(39) Michalkiewicz, B.; Majewska, J.; Kądziołka, G.; Bubacz, K.; Mozia, S.; Morawski, A. W. Reduction of CO2 by adsorption and reaction on surface of TiO2-nitrogen modified photocatalyst. *J. CO2 Util.* **2014**, *5*, 47−52.
(40) Karl, T. R.; Trenberth, K. E. Modern global climate change. *Science* **2003**, *302*, 1719−1723.
(41) Royer, S.; Duprez, D. Catalytic Oxidation of Carbon Monoxide over Transition Metal Oxides. *ChemCatChem* **2011**, *3*, 24−65.
(42) Fujita, T.; Ishida, T.; Shibamoto, K.; Honma, T.; Ohashi, H.; Murayama, T.; Haruta, M. CO Oxidation over Au/ZnO: Unprecedented Change of the Reaction Mechanism at Low Temperature Caused by a Different O2 Activation Process. *ACS Catal.* **2019**, *9*, 8364−8372.
(43) Shi, H.; Yuan, H.; Ruan, S.; Wang, W.; Li, Z.; Li, Z.; Shao, X. Adsorption and Diffusion of CO on Clean and CO2-Precovered ZnO($10\bar{1}0$). *J. Phys. Chem. C* **2018**, *122*, 8919−8924.
(44) Nugraha; Saputro, A. G.; Agusta, M. K.; Yuliarto, B.; Dipojono, H. K.; Rusydi, F.; Maezono, R. Selectivity of CO and NO adsorption on ZnO (0002) surfaces: A DFT investigation. *Appl. Surf. Sci.* **2017**, *410*, 373−382.
(45) Xu, J.; Xue, Z.; Qin, N.; Cheng, Z.; Xiang, Q. The crystal facet-dependent gas sensing properties of ZnO nanosheets: Experimental and computational study. *Sens. Actuators, B* **2017**, *242*, 148−157.
(46) Huang, M. H.; Mao, S.; Feick, H.; Yan, H.; Wu, Y.; Kind, H.; Weber, E.; Russo, R.; Yang, P. Room-temperature ultraviolet nanowire nanolasers. *Science* **2001**, *292*, 1897−1899.
(47) Wan, Q.; Li, Q. H.; Chen, Y. J.; Wang, T. H.; He, X. L.; Li, J. P.; Lin, C. L. Fabrication and ethanol sensing characteristics of ZnO nanowire gas sensors. *Appl. Phys. Lett.* **2004**, *84*, 3654−3656.
(48) Liao, L.; Lu, H. B.; Li, J. C.; He, H.; Wang, D. F.; Fu, D. J.; Liu, C.; Zhang, W. F. Size Dependence of Gas Sensitivity of ZnO Nanorods. *J. Phys. Chem. C* **2007**, *111*, 1900−1903.
(49) Klier, K. Methanol Synthesis. *Adv. Catal.* **1982**, *31*, 243−313.
(50) Fujita, S.-i.; Ito, H.; Takezawa, N. Methanol Synthesis from CO2and H2over a ZnO Catalyst. Effect of the Pretreatment with CO−H2upon the Reaction. *Bull. Chem. Soc. Jpn.* **1993**, *66*, 3094−3096.
(51) Wang, Y.; Kovacik, R.; Meyer, B.; Kotsis, K.; Stodt, D.; Staemmler, V.; Qiu, H.; Traeger, F.; Langenberg, D.; Muhler, M.; Woll, C. CO2 activation by ZnO through the formation of an unusual tridentate surface carbonate. *Angew. Chem., Int. Ed.* **2007**, *46*, 5624−5627.
(52) Kühnle, A. Self-assembly of organic molecules at metal surfaces. *Curr. Opin. Colloid Interface Sci.* **2009**, *14*, 157−168.
(53) Solymosi, F. The bonding, structure and reactions of CO2 adsorbed on clean and promoted metal surfaces. *J. Mol. Catal.* **1991**, *65*, 337−358.
(54) Freund, H. J.; Roberts, M. W. Surface chemistry of carbon dioxide. *Surf. Sci. Rep.* **1996**, *25*, 225−273.
(55) Heß, G.; Baumgartner, C.; Froitzheim, H. Adsorption sites and microstructures ofCO2on Fe(111) derived from specular and off-specular HREELS. *Phys. Rev. B* **2001**, *63*, No. 165416.
(56) Ford, R. R.Carbon Monoxide Adsorption on the Transition Metals. In *Advances in Catalysis*; Elsevier, 1970; Vol. *21*, pp 51−150.
(57) Rodrigues, N. M.; Martins, J. B. L. Theoretical evaluation of the performance of IRMOFs and M-MOF-74 in the formation of 5-fluorouracil@MOF. *RSC Adv.* **2021**, *11*, 31090−31097.
(58) Li, W.; Yang, H.; Jiang, X.; Liu, Q. Highly selective CO 2 adsorption of ZnO based N-doped reduced graphene oxide porous nanomaterial. *Appl. Surf. Sci.* **2016**, *360*, 143−147.
(59) Cheng, W. H.; Kung, H. H. Interaction of CO, CO2 and O2 with nonpolar, stepped and polar Zn surfaces of ZnO. *Surf. Sci.* **1982**, *122*, 21−39.
(60) Wang, Y.; Xia, X.; Urban, A.; Qiu, H.; Strunk, J.; Meyer, B.; Muhler, M.; Woll, C. Tuning the reactivity of oxide surfaces by charge-accepting adsorbates. *Angew. Chem., Int. Ed.* **2007**, *46*, 7315−7318.
(61) Bolis, V.; Fubini, B.; Giamello, E.; Reller, A. Effect of form of the surface reactivity of differently prepared zinc oxides. *J. Chem. Soc., Faraday Trans. 1* **1989**, *85*, 855−867.
(62) Gay, R. R.; Nodine, M. H.; Henrich, V. E.; Zeiger, H. J.; Solomon, E. I. Photoelectron study of the interaction of carbon monoxide with zinc oxide. *J. Am. Chem. Soc.* **1980**, *102*, 6752−6761.
(63) Hotan, W.; Göpel, W.; Haul, R. Interaction of CO2 and co with nonpolar zinc oxide surfaces. *Surf. Sci.* **1979**, *83*, 162−180.
(64) Abrahams, S. C.; Bernstein, J. L. Remeasurement of the structure of hexagonal ZnO. *Acta Crystallogr., Sect. B: Struct. Crystallogr. Cryst. Chem.* **1969**, *25*, 1233−1236.
(65) Martins, J. B. L.; Andrés, J.; Longo, E.; Taft, C. A. A theoretical study of (1010) and (0001) ZnO surfaces: molecular cluster model, basis set and effective core potential dependence. *J. Mol. Struct.:THEOCHEM* **1995**, *330*, 301−306.
(66) Marana, N. L.; Longo, V. M.; Longo, E.; Martins, J. B.; Sambrano, J. R. Electronic and structural properties of the (1010) and (1120) ZnO surfaces. *J. Phys. Chem. A* **2008**, *112*, 8958−8963.
(67) Beltrán, A.; Andrés, J.; Calatayud, M.; Martins, J. B. L. Theoretical study of ZnO (1010) and Cu/ZnO (1010) surfaces. *Chem. Phys. Lett.* **2001**, *338*, 224−230.
(68) Farias, S. A. S.; Longo, E.; Gargano, R.; Martins, J. B. CO2 adsorption on polar surfaces of ZnO. *J. Mol. Model.* **2013**, *19*, 2069−2078.
(69) Schaftenaar, G.; Noordik, J. H. Molden: a pre- and post-processing program for molecular and electronic structures. *J. Comput.-Aided Mol. Des.* **2000**, *14*, 123−134.
(70) Frisch, M. J.; H -G, M.; Trucks, G. W.; Foresman, J. B.; Raghavachari, K.; Schlegel, H. B.; Robb, M.; Binkley, J. S.; Gonzalez, C.; Defrees, D. J.; Fox, D. J.; Whiteside, R. A.; Seeger, R.; Melius, C. F.; Baker, J.; Kahn, L. R.; Stewart, J. J. P.; Fluder, E. M.; Topiol, S.; Pople, J. A. *Gaussian Program*, 1990.
(71) Dubbeldam, D.; Calero, S.; Ellis, D. E.; Snurr, R. Q. RASPA: molecular simulation software for adsorption and diffusion in flexible nanoporous materials. *Mol. Simul.* **2016**, *42*, 81−101.
(72) Wilmer, C. E.; Kim, K. C.; Snurr, R. Q. An Extended Charge Equilibration Method. *J. Phys. Chem. Lett.* **2012**, *3*, 2506−2511.
(73) Stenberg, S.; Stenqvist, B. An Exact Ewald Summation Method in Theory and Practice. *J. Phys. Chem. A* **2020**, *124*, 3943−3946.
(74) Stewart, J. J. P. MOPAC: A General Molecular Orbital Package. *Quant. Chem. Prog. Exch.* **1990**, *10*, No. 86.

https://doi.org/10.1021/acsomega.3c06378
ACS Omega 2023, 8, 46830−46840